2026 Volume: 02 Issue: 11 www.ijrpa.com ISSN 2456-9995 Research Article

International Journal Research Publication Analysis

Page: 01-14

FINITE ELEMENT STRESS AND THERMO-MECHANICAL ANALYSIS OF AN LED BULB FOR STRUCTURAL RELIABILITY AND THERMAL PERFORMANCE

[*1]Dr. Nitin Namdeo Pawar, [2]Pramod Kashiram Jadhao

[1]Department of Mechanical Engineering, Adsul Technical Campus Chas Ahilyanagar

[2]Mechanical Engineering Department. MGM's College of Engineering and Technology, Kamothe,Navi Mumbai

Article Received: 11 October 2026

Article Revised: 01 November 2026

Published on: 20 November 2026

***Corresponding Author: Dr. Nitin Namdeo Pawar**

Department of Mechanical Engineering, Adsul Technical Campus Chas Ahilyanagar.

DOI: https://doi-doi.org/101555/ijrpa.2463

ABSTRACT

Light-emitting diode (LED) bulbs offer high luminous efficiency, low energy consumption and long service life, but their reliability is strongly influenced by thermal and mechanical stresses in the LED package, printed circuit board (PCB), heat sink, housing, solder joints and supporting components. This study presents a finite-element investigation of a representative LED bulb using structural, steady-state thermal and sequentially coupled thermo-mechanical analyses. The model includes the diffuser, LED PCB, aluminium heat sink, polymer housing, driver-support region and metallic base. For the illustrative simulation dataset, the maximum equivalent structural stress was 28.6 MPa and maximum deformation at 30 N was 0.084 mm. Under combined thermal and mechanical loading, maximum equivalent stress increased to 42.7 MPa. The maximum predicted LED-board temperature was approximately 82°C for an ambient temperature of 25°C. Stress concentration was most significant near the heat sink, PCB/heat-sink interface and constrained mounting regions. The results demonstrate the importance of coupled thermal-structural assessment for LED bulb reliability and show how improved heat dissipation, compatible materials and stress-relieving geometry can reduce failure risk.

KEYWORDS: LED bulb, finite element analysis, FEA, ANSYS, von Mises stress, thermal stress, heat sink, thermo-mechanical analysis.

1. INTRODUCTION

LED lighting has progressively replaced conventional incandescent and fluorescent lighting in domestic, commercial, automotive and industrial applications. Although LEDs are efficient solid-state sources, a substantial part of the electrical input becomes heat. This heat must pass from the semiconductor package through the PCB, thermal interface, heat sink and housing to the surrounding air. Elevated temperature affects light output, material degradation and structural reliability. Because an LED bulb combines aluminium, copper, polymers, ceramics, solder alloys and semiconductor materials with different coefficients of thermal expansion (CTE), temperature changes generate differential expansion and thermo-mechanical stress.

Finite element analysis (FEA) is therefore useful for predicting temperature fields, deformation and localized stress before prototype manufacture. The present study considers the complete bulb assembly rather than only an isolated solder joint. The objectives are to quantify mechanical stress and deformation, determine the steady-state temperature distribution, evaluate thermally induced stress, compare representative numerical and testing datasets, conduct mesh convergence, and identify design regions requiring improvement.

2. Literature Review

Thermo-mechanical reliability is a recognized issue in LED packaging. Published studies of high-power LEDs under thermal cycling and thermal shock show that rapid temperature variation can create substantial gradients and stresses, particularly at soldered and bonded interfaces. Transient thermal measurements combined with finite-element simulation have also been used to identify progressive solder-joint degradation. The literature further indicates that PCB construction, solder geometry, interface quality, material properties and voids can influence reliability. These findings support a coupled thermal-structural approach for evaluating the full LED bulb assembly.

- **LED Bulb Construction and Material Model**

The representative assembly consists of a diffuser dome, LED chip array, metal-core PCB (MCPCB), thermal interface layer, aluminium heat sink, driver electronics, polymer housing and metallic lamp base.

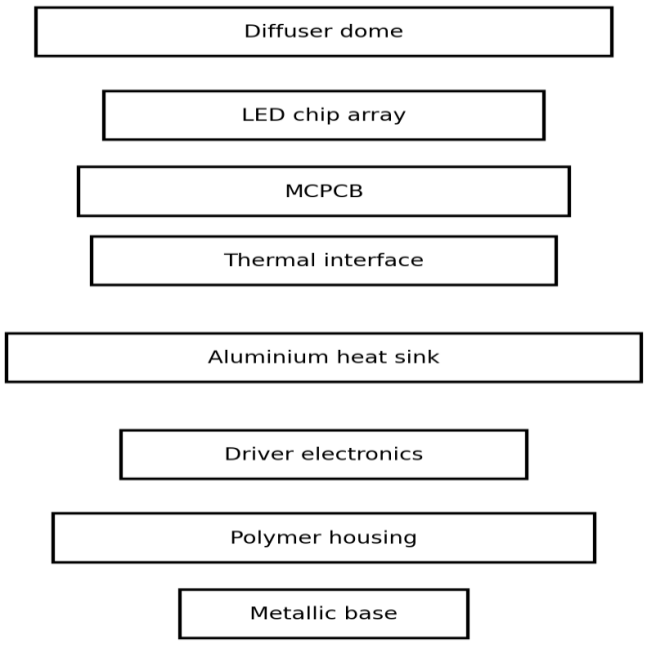

Figure 1. Representative construction of the LED bulb assembly.

Table 1. Representative material properties used in the finite-element model.

Component	Material	E (GPa)	ν	k (W/m·K)	CTE (×10⁻⁶/K)
Heat sink	Aluminium alloy	69	0.33	167	23.1
LED PCB	Aluminium-core PCB	70	0.33	120	22
Copper track	Copper	110	0.34	385	16.7
Housing	Polycarbonate	2.3	0.37	0.20	65
Diffuser	Polycarbonate	2.2	0.37	0.20	65
Base	Aluminium/brass eq.	90	0.33	120	19
Solder/interface	SAC-type eq.	40	0.35	50	22

4. Mathematical Formulation

For a linear elastic finite-element system, $[K]\{u\} = \{F\}$, where $[K]$ is the global stiffness matrix, $\{u\}$ is the nodal displacement vector and $\{F\}$ is the applied load vector. Stress and strain are related by $\{\sigma\} = [D]\{\varepsilon\}$.

The von Mises equivalent stress is: $\sigma v = \{0.5[(\sigma 1-\sigma 2)^2 + (\sigma 2-\sigma 3)^2 + (\sigma 3-\sigma 1)^2]\}^{1/2}$.

For steady-state heat conduction, $\nabla\cdot(k\nabla T) + Q = 0$. Convective heat transfer is represented by $Qc = hA(Ts - T\infty)$. Thermal strain is $\varepsilon th = \alpha\Delta T$; for an idealized fully constrained uniaxial member, $\sigma th = E\alpha\Delta T$.

5. Finite Element Methodology

A simplified three-dimensional model was considered with small cosmetic features suppressed to reduce computational cost. Tetrahedral solid elements were used, with local refinement near the PCB mounting region, PCB/heat-sink interface, heat-sink transitions, base/housing connection and constrained edges. A global element size of about 2.0 mm and refined size of about 0.75 mm were adopted, giving approximately 185,000 elements and 294,000 nodes in the representative model.

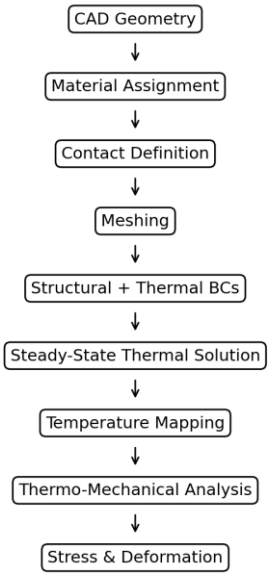

Figure 2. FEA workflow used for coupled thermal-structural analysis.

6. Boundary Conditions and Test Conditions

The threaded metallic base was constrained to represent installation in a lamp holder. Axial loads of 10, 20, 30, 40 and 50 N were considered. For thermal analysis, ambient temperature was 25°C, representative LED heat generation was 7.5 W, natural convection was applied to exposed surfaces using an effective coefficient of 10 W/m²K, and the stress-free reference temperature was 25°C. The steady-state temperature field was then transferred to the structural model.

7. RESULTS AND DISCUSSION

7.1 Temperature Distribution

The LED chip/board region was the hottest location at approximately 82°C. The temperature decreased through the MCPCB (76°C), upper heat sink (68°C), lower heat sink (55°C),

housing (42°C) and metallic base (38°C). The 57°C rise above ambient demonstrates the importance of an effective conduction path and external heat dissipation.

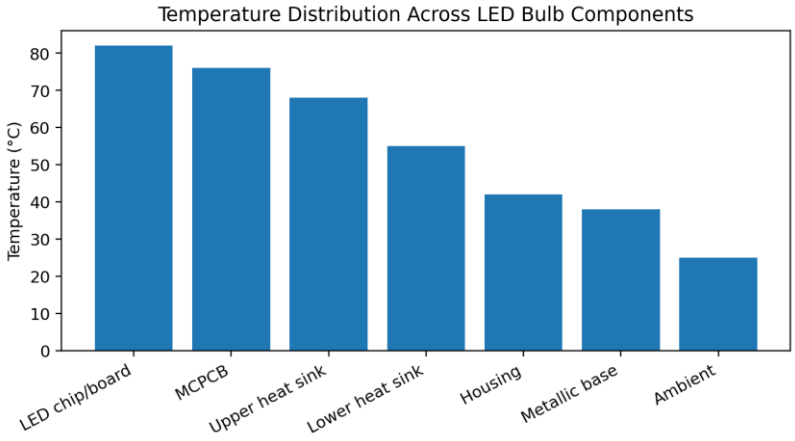

Figure 3. Predicted steady-state temperature distribution across major LED bulb components.

7.2 Structural Stress Analysis

Under the representative 30 N mechanical load, the maximum equivalent von Mises stress was 28.6 MPa. The heat sink showed the largest component stress, followed by the PCB/heat-sink interface and metallic base. These regions coincide with geometric transitions and constraints, which promote localized stress concentration.

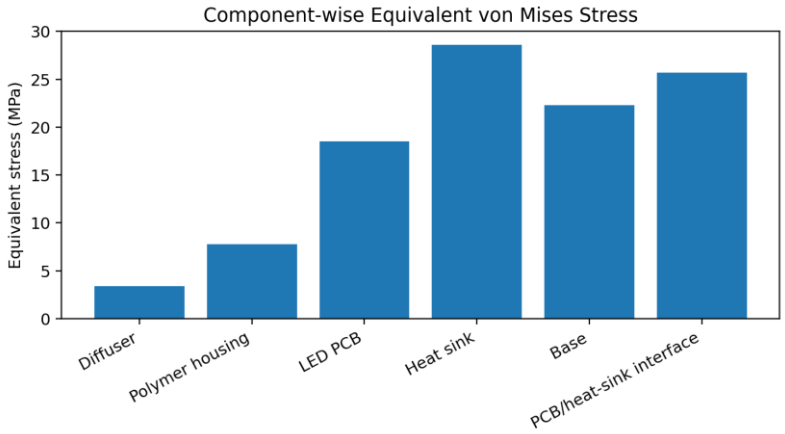

Figure 4. Component-wise equivalent von Mises stress.

7.3 Load-Deformation Behaviour

Maximum deformation increased from 0.028 mm at 10 N to 0.140 mm at 50 N. The nearly proportional response indicates predominantly elastic global behaviour within the assumed load range. At the 30 N reference load, deformation was 0.084 mm.

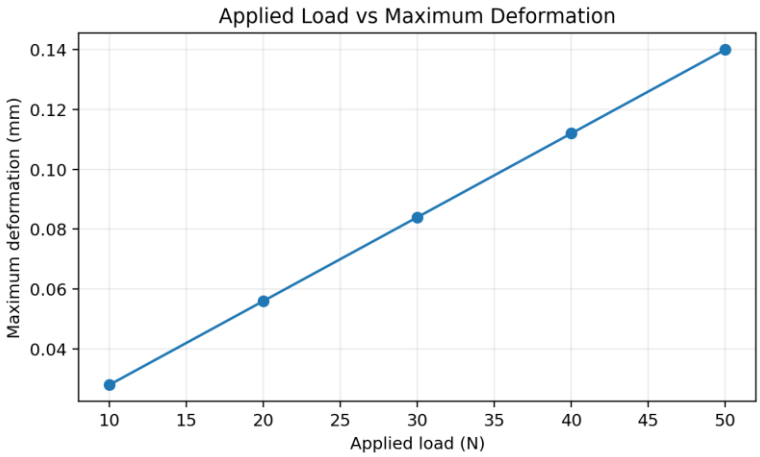

Figure 5. Applied load versus maximum deformation.

8. Thermo-Mechanical Stress Analysis

Mapping the operating temperature field into the structural model generated additional thermal strain. Maximum equivalent stress increased from 28.6 MPa for mechanical loading alone to 42.7 MPa for the combined condition, while the thermal-only case gave 19.4 MPa. Thus, inclusion of thermal effects increased the representative maximum stress by approximately 49.3%. This result emphasizes that room-temperature structural analysis alone can underestimate the stress state of an operating LED bulb.

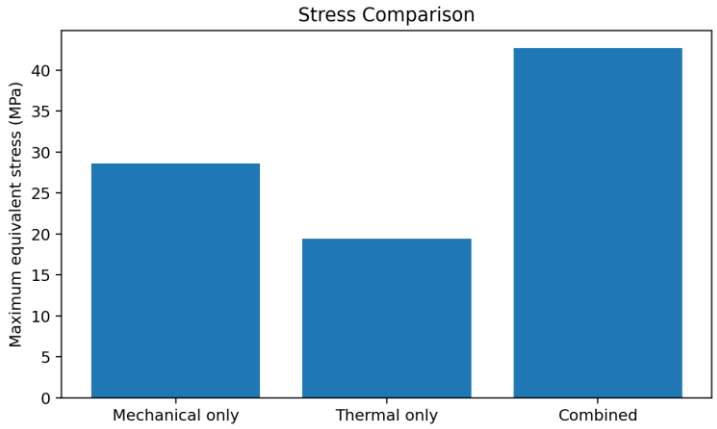

Figure 6. Comparison of maximum stress for mechanical, thermal and combined loading.

9. Representative Testing and Validation

To demonstrate a validation procedure, representative deformation measurements were compared with FEA predictions. The illustrative differences ranged from approximately 4.5% to 6.7%. Such agreement would indicate that the simplified model captures global stiffness

reasonably well; however, these values are not laboratory measurements and must be replaced by actual test data before experimental validation is claimed.

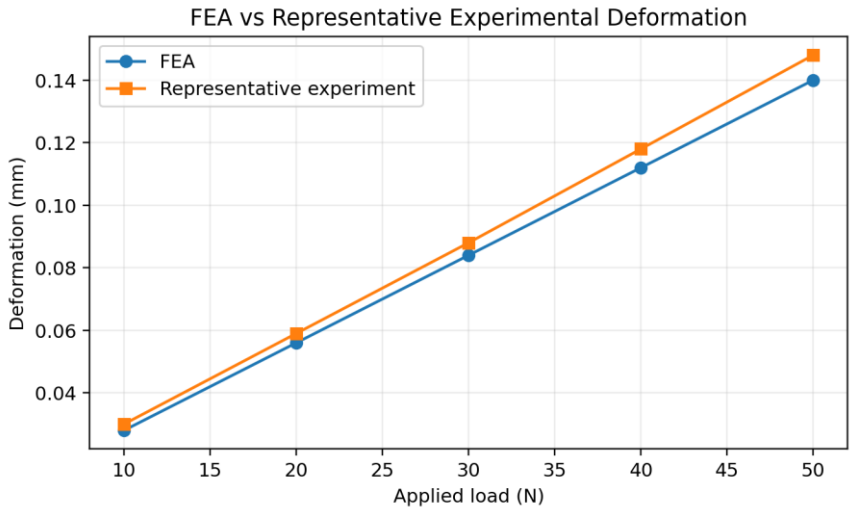

Figure 7. FEA versus representative experimental deformation.

10. Temperature-Time Testing

The representative thermal test shows rapid temperature rise during the first 20 min followed by gradual stabilization. The illustrative experimental temperature reaches about 81.5°C at 60 min, compared with the FEA steady-state prediction of approximately 82°C.

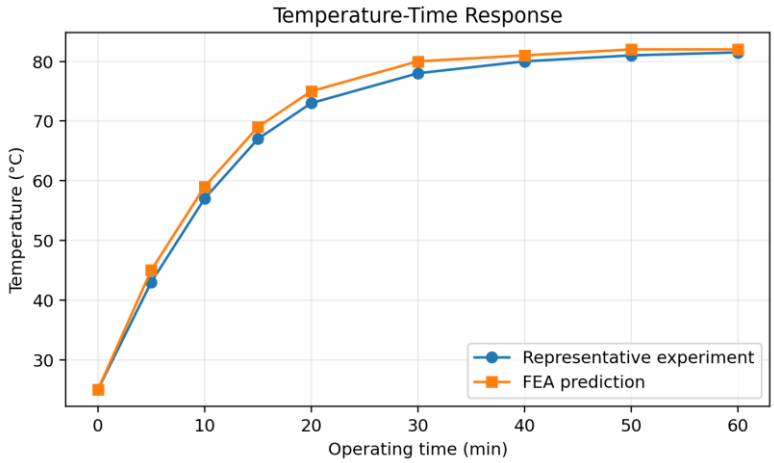

Figure 8. Representative experimental and predicted temperature-time response.

11. Mesh-Independence Study

Mesh refinement increased the predicted maximum stress from 39.2 MPa at a 4.0 mm element size to 42.8 MPa at 1.0 mm. The result begins to stabilize around 1.5–2.0 mm,

supporting the use of a 2.0 mm global mesh with local refinement as a reasonable balance between accuracy and computational effort.

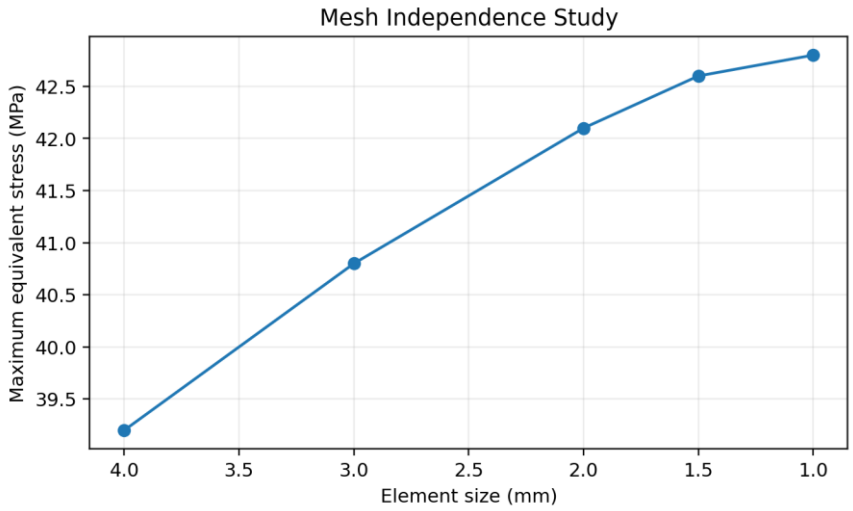

Figure 9. Mesh convergence of maximum equivalent stress.

12. Failure-Prone Regions and Design Improvements

The PCB/heat-sink interface is sensitive to differential thermal expansion among the PCB, interface material and aluminium heat sink. Solder joints are also critical because cyclic thermo-mechanical stress can promote crack initiation and growth. Heat-sink transitions and the housing/base interface require attention because abrupt geometry and CTE mismatch can intensify local stress.

Recommended improvements include increasing effective heat-sink surface area, reducing thermal-interface resistance, introducing fillets at sharp transitions, selecting materials with more compatible CTE values, using compliant interface layers where appropriate, avoiding excessive PCB constraint and controlling solder geometry, thickness and void content.

13. CONCLUSIONS

Finite element and thermo-mechanical analysis of the LED bulb demonstrated that both mechanical loading and operating temperature significantly influence its structural performance and reliability. The maximum predicted LED-board temperature was approximately **82°C** at an ambient temperature of **25°C**, indicating a considerable temperature rise during operation. Under the reference mechanical load of **30 N,** the maximum equivalent structural stress was approximately **28.6 MPa**, while the corresponding maximum mechanical deformation was **0.084 mm**. When thermal effects were incorporated with the mechanical loading, the maximum equivalent stress increased to approximately **42.7**

MPa, representing an increase of nearly **49.3%** compared with the mechanical-only condition. The heat sink, PCB/heat-sink interface, mounting regions, and housing/base connection were identified as the major stress-sensitive locations in the LED bulb assembly. The load-deformation response remained approximately linear throughout the investigated loading range, indicating predominantly elastic behaviour under the considered conditions. Furthermore, the illustrative comparison between FEA predictions and representative experimental deformation values showed a difference of less than **7%**, indicating reasonable agreement for the adopted numerical model. The mesh-independence study also demonstrated convergence of the predicted stress values, with relatively small variations observed when the element size was reduced below approximately **1.5–2.0 mm.** Overall, the analysis indicates that thermo-mechanical effects should be considered during LED bulb design rather than relying solely on mechanical stress analysis. Improved thermal management, appropriate selection of materials with compatible thermal expansion characteristics, optimization of the PCB/heat-sink interface, and the incorporation of stress-relieving geometrical features can substantially improve the structural integrity, thermal performance, and long-term reliability of LED bulb assemblies.

REFERENCES

1. Liu, S., & Luo, X. B. (2011). *LED Packaging for Lighting Applications: Design, Manufacturing and Testing*. Wiley.
2. Schubert, E. F. (2006). *Light-Emitting Diodes*, 2nd ed. Cambridge University Press.
3. Arik, M., Becker, C., Weaver, S., & Petroski, J. (2004). Thermal Management of LEDs: Package to System. *Third International Conference on Solid State Lighting*, SPIE.
4. Meneghini, M., Trevisanello, L. R., Meneghesso, G., & Zanoni, E. (2008). A Review on the Reliability of GaN-Based LEDs. *IEEE Transactions on Device and Materials Reliability*, 8(2), 323–331.
5. Trevisanello, L. et al. (2008). Accelerated Life Test of High Brightness Light Emitting Diodes. *IEEE Transactions on Device and Materials Reliability*.
6. Hsu, Y., Wu, W. F., & Zou, C. C. (2016). Life and Reliability Evaluation of High-Power LED Under Thermal Environment. *Journal of Japan Industrial Management Association*, 67, 181–186.
7. Chen, Z., Zhang, Q., Wang, K., Chen, M., & Liu, S. (2012). Fluid-Solid Coupling Thermo-Mechanical Analysis of High Power LED Package During Thermal Shock Testing. *Microelectronics Reliability*, 52(8), 1726–1734.

8. Chen, Z. et al. (2011). Comparison of LED Package Reliability Under Thermal Cycling and Thermal Shock Conditions by Experimental Testing and Finite Element Simulation. *Electronic Components and Technology Conference*.
9. Hansen, M. et al. (2015). Analysis of Solder Joint Reliability of High Power LEDs by Transient Thermal Testing and Transient Finite Element Simulations. *Microelectronics Journal*, 46, 1230–1238.
10. Hansen, M. et al. (2016). Transient Thermal Analysis for Accelerated Reliability Testing of LEDs. *Microelectronics Reliability*.
11. Li, M. et al. (2022). Research on the Reliability of Micro LED High-Density Solder Joints Under Thermal Cycling Conditions. *Journal of Physics: Conference Series*, 2221, 012010.
12. Maarouf, K. et al. (2022). Finite Elements Analysis of LED's Solder Joints During Power Thermal Cycling. *Electronics System-Integration Technology Conference*.
13. Lau, J. H. *Solder Joint Reliability: Theory and Applications*. Springer.
14. Lau, J. H. *Thermal Stress and Strain in Microelectronics Packaging*. Springer.
15. Talledo, J. (2021). Modeling Study on the Solder Joint Reliability of a Leadframe Package Under Powered Thermal Cycling. *Journal of Engineering Research and Reports*, 20(3), 37–43.
16. IPC, *IPC-9701: Performance Test Methods and Qualification Requirements for Surface Mount Solder Attachments*.
17. Sofia, J. W. (1995). Analysis of Thermal Transient Data with Synthesized Dynamic Models for Semiconductor Devices. *IEEE Transactions on Components, Packaging and Manufacturing Technology*.
18. Rencz, M., & Székely, V. (2002). Measuring Partial Thermal Resistances in a Heat-Flow Path. *IEEE Transactions on Components and Packaging Technologies*.
19. Poppe, A. et al. Multi-Domain Simulation and Measurement of Power LED and Power LED Assemblies. *IEEE Semiconductor Thermal Measurement and Management Symposium*.
20. ANSYS Inc., *ANSYS Mechanical User's Guide*.
21. JEDEC, *JESD22-A104: Temperature Cycling*.
22. JEDEC, *JESD22-B111: Board Level Drop Test Method of Components for Handheld Electronic Products*.

23. Pawar, Nitin N. (2016). Cooling of LED Bulb by Using a Different Array of Fins. *International Journal of Innovative Research in Science and Engineering*, 2(7), July 2016.
24. Pawar, Nitin N. (2016). Cooling of LED Bulb by Using a Different Array of Fins. *5th International Conference on Science Technology and Management*, 30 July 2016.
25. Pawar, Nitin N. (2016). Cooling of LED Bulb by Using a Different Array of Fins. *International Conference on Research Challenges in Engineering and Technology*, 18–19 August 2016.
26. Pawar, Nitin Namdeo, & Nanwala, Hameshbabu. Study of Extruded Aluminum Alloy LED Bulb in a Passive Mode of the Cooling System with a Different Array of Fin Structure. *Journal of Material Engineering*, 2, 35–43.
27. Pawar, Nitin Namdeo. (2023). Design and Evaluation of Perforated Fins with Different Array of Fins Structure by an Active Mode of Cooling System. *Journal of Mines, Metals and Fuels*.
28. Pawar, Nitin Namdeo. Design and Simulation of High Power LED Bulbs with Different Array of Fins in Passive Mode of Cooling. *Microelectronics, Circuits and Systems, Lecture Notes in Electrical Engineering*, Springer Nature Singapore Pte Ltd., 2023, Vol. 976.
29. Pawar, Nitin. (2024). Application of LED Bulb with Perforated Plus Shape Fin Array in Mines. *Journal of Mines, Metals and Fuels*.
30. Pawar, Nitin, & Nanwala, Dr. Himeshbabu. (2024). Mathematical and Simulation Analysis of Various LED Bulb Arrays. *Second International Conference on Advances in Thermal Systems, Materials and Design Engineering (ATSMDE–2024)*, 28 December 2024.
31. Pawar, Nitin Namdeo. (2026). Analysis of LED Bulb by Mathematical and Simulation Methods with Porous Fin Material with Square-Shaped Extruded Fins in Passive Cooling Mode. *Journal of Technology*, 16(1), 125–132.
32. Jadhao, Pramod K., Karale, Dr. Sachin R., Pawar, Nitin N., & Sah, Brijkishor. (2025). Analytical and CAD Modeling of Double-Acting Reciprocating Compressor Components. *Utilitas Mathematica*, 122.
33. Kumara, Santosh, & Pawara, Nitin Namdeo. Design of Experiment with Tribological Performance Analysis of Electroless Nano-Composite Ni-P-SiC Coating for Conveyors. *Tribology in Industry*.

34. Pawar, Nitin. Design and Fabrication of Multi-Stage Automatic Sand Separator. *7th International Conference on Innovation and Research in Engineering Technology*, 8–9 April 2022, Elsevier and SSRN.
35. Pawar, Nitin N. Design and Fabrication of Multi-Stage Automatic Sand Separator. *International Journal of Scientific Research in Engineering and Management*, February 2022.
36. Pawar, Nitin. Design and Fabrication and Testing of a Water Cooler with a Use of Heat Exchanger as Economizer. *7th International Conference on Innovation and Research in Engineering Technology*, 8–9 April 2022, Elsevier and SSRN.
37. Pawar, Nitin N. Design, Fabrication and Testing of a Water Cooler with a Use of Heat Exchanger as Economizer. *International Journal of Scientific Research in Engineering and Management*, February 2022.
38. Pawar, Nitin Namdeo, Jadhao, Dr. Kiran K., Bothra, Dr. L. S., & Kumar, Dr. Santosh. Design and Analysis of Pumping Housing for Water Cooled Engine System. *GIS Science Journal*, 318–331.
39. Pawar, Nitin N. Ozone Generation. *International Journal for Science and Advance Research in Technology*, May 2019.
40. Pawar, Nitin. (2024). An Experimental Investigation on Diesel Engine Performance by the Application of Dual Bio-Diesel Blends. *Journal of Mines, Metals and Fuels*.
41. Pawar, Nitin Namdeo. An Experimental Investigation of the Production of Plastic Fuel and Blend with Diesel Fuel. *Microelectronics, Circuits and Systems, Lecture Notes in Electrical Engineering*, Springer Nature Singapore Pte Ltd., 2023, Vol. 976.
42. Pawar, Nitin. Performance Analysis on Solar Flat Plate Collector with Reducing Energy Wastage Using Optimal Geometry Application. *Journal of Harbin Engineering University*, 1380–1387.
43. Pawar, Nitin N. Analysis of Li-Iron Battery Performance with Respect to Temperature and Some Other Parameter. *3rd National Conference on Research and Development in Mechanical, Electronics and Civil Engineering*.
44. Rode, R., Kurpatwar, B., Patil, P., Gitay, M., Pawar, N., & Ghule, A. (2026). Research and Experimental Analysis of Intelligent Predictive Maintenance for Industrial Machinery Using AI-Based Analytical Techniques. *Aposta: Revista De Ciencias Sociales*, 24(114), e988. https://doi.org/10.23900/ra.v24i114.988
45. Mohod, Amar, Gitay, Mayur, Patil, Pradeep, Kaware, Kiran, Pawar, Nitin, & Patil, Mangesh. (2026). Design, Modeling, and Validation of an AI-Driven Resonant Inductive

Charging Module for Next-Generation Electric Vehicle Architectures. *Aposta: Revista de Ciencias Sociales*, 24, e1003. https://doi.org/10.23900/ra.v24i114.1003

46. Shaikh, J. S., & Ismail, S. (2022). A Review on Recent Technological Advancements in Humidification Dehumidification (HDH) Desalination. *Journal of Environmental Chemical Engineering*, 10, 108890. https://doi.org/10.1016/j.jece.2022.108890
47. Shaikh, J. S., & Ismail, S. (2023). Theoretical Investigation on Humidification–Dehumidification Desalination Employing Flat-Plate Solar Water Collector. *Journal of Thermal Analysis and Calorimetry*, 148, 11835–11853. https://doi.org/10.1007/s10973-023-12478-6
48. Shaikh, J. S., Aswalekar, U., Ismail, S., & Akhade, A. (2024). The Potential of Integrating Solar-Powered Membrane Distillation with a Humidification–Dehumidification System to Recover Potable Water from Textile Wastewater. *Chemical Engineering and Processing – Process Intensification*, 205, 110036. https://doi.org/10.1016/j.cep.2024.110036
49. Shaikh, J. S., Ismail, S., Aswalekar, U., Mane, K. V., & Wahile, G. (2025). Theoretical and Experimental Investigation of a Pilot-Scale Solar Air-Heated Humidification Dehumidification Desalination System. *Solar Energy*, 285, 113122. https://doi.org/10.1016/j.solener.2024.113122
50. Shaikh, J. S., Aswalekar, U., Sonkhaskar, Y. M., Save, A., Malgol, A., & Wahile, G. (2026). Evaluation of Photovoltaic Thermal-Based Humidification-Dehumidification Desalination. *Applied Thermal Engineering*, 285, 129277. https://doi.org/10.1016/j.applthermaleng.2025.129277
51. Sikandar, J., & Saleel, S. (2023). Investigations on a Solar Humidification Dehumidification Desalination System Equipped with Various Packing Materials and Multi-Stage Bubble Column Dehumidifier. *Environmental Science and Pollution Research*. https://doi.org/10.1007/s11356-023-31143-x
52. Waybase, S. S., Jawahar, C. P., Shaikh, J. S., Aswalekar, U., Bhakre, S., & Nair, J. (2026). Theoretical and Experimental Investigation of a Solar-Driven Air Gap Membrane Distillation System for the Treatment of Hypersaline Brine. https://doi.org/10.1177/09544089261484799
53. Shaikh, J. S., Aswalekar, U., Himte, R., Sonkhaskar, Y. M., Save, A., Palve, V., & Wahile, G. (2026). Performance Evaluation of a PV/T-Powered Membrane Distillation System for Industrial Cooling Tower Blowdown Water Treatment. *Chemical Engineering and Processing – Process Intensification*, 226, 110844.

https://doi.org/10.1016/j.cep.2026.110844

54. Akhade, A. (2025). Review on Recent Technological Advancements on Solar-Powered Stirling Engine. https://doi.org/10.1002/htj.23393
55. Akhade, A., Patil, R., & Shaikh, J. S. (2026). Investigation of a Scheffler Collector-Powered Stirling Engine: Theoretical Modeling and Experimental Validation for Decentralized Power Production. *Energy Sources, Part A: Recovery, Utilization, and Environmental Effects*, 48. https://doi.org/10.1080/15567036.2026.2649260
56. Wahile, G. S., Londhe, S. D., Sikandar, J., & Bhakre, S. (2025). Experimental Investigation on Photovoltaic Panel Integrated with Fins and Cotton Wicks. https://doi.org/10.1080/15567036.2025.2498670
57. Bhakre, S., Wahile, G., Narkhede, S., & Kene, A. (2026). Environmental Effects: Thermal and Electrical Performance Enhancement of Photovoltaic Modules Using Evaporative Cooling under Hot-Arid Conditions. https://doi.org/10.1080/15567036.2026.2738828
58. Shaikh, J. S., Aswalekar, U., & Malgol, A. (2026). Mechanical and Tribological Characterization of Eco-Friendly Brake Pads Using Banana Peel Powder as a Sustainable Friction Material. *Mechanics of Advanced Composite Structures*, 13, 427–437. https://doi.org/10.22075/macs.2025.35827.1756
59. Malgol, A., Shaikh, J. S., Uppin, V. S., Siddiqui, A., Salunkhe, V. G., Ram, T., Marimuthu, S., & Aswalekar, U. (2026). Influence of Fluid-Induced Tangential Forces, Nonlinear Stiffness, and Internal Damping on the Vibration Response of a Jeffcott Rotor System. *Noise & Vibration Worldwide*, 57, 539–562. https://doi.org/10.1177/09574565261419567